Applied Catalysis B: Environmental 144 (2014) 809–815

Contents lists available at ScienceDirect

Applied Catalysis B: Environmental

journal homepage: www.elsevier.com/locate/apcatb

Selective catalytic reduction of NO using acetone solvent vapors as the reducing agent over Cu^{2+} and/or Al^{3+} ions substituted MCM-41 catalysts

Mani Karthik[a,b,*], Hsunling Bai[b]

[a] CIC Energigune, Parque Tecnológico, C/ Albert Einstein 48, 01510 Miñano, Álava, Spain
[b] Institute of Environmental Engineering, National Chiao Tung University, Hsinchu 300, Taiwan

ARTICLE INFO

Article history:
Received 18 April 2013
Received in revised form 31 July 2013
Accepted 7 August 2013
Available online 28 August 2013

Keywords:
Selective catalytic reduction
Cu–Al–MCM-41
Metal oxides
Nitrogen oxides abatement
Acetone

ABSTRACT

Selective catalytic reduction (SCR) of nitrogen monoxide (NO) using acetone solvent vapors as the reducing agent over mesoporous Cu–MCM-41, Al–MCM-41, Cu–Al–MCM-41 and CuO supported metal oxides such as CuO/Al_2O_3 and CuO/SiO_2 was investigated in this study. The synthesized materials were characterized by using powder low-angle X-ray diffraction (XRD), N_2 adsorption–desorption measurements, ^{27}Al magic angle spinning-nuclear magnetic resonance spectroscopy (MAS-NMR), electron paramagnetic resonance spectroscopy (EPR) and inductively coupled plasma-mass spectrometer (ICP-MS) analysis. The presence of isolated Cu^{2+} ions and tetrahedrally coordinated Al^{3+} ions within the framework of Cu–Al–MCM-41 catalyst played a vital role in this deNO*x* reaction as confirmed by EPR and ^{27}Al MAS-NMR spectroscopic studies, respectively. Among the various catalysts studied, bifunctional Cu–Al–MCM-41 was found to be the most effective catalyst for achieving maximum deNO*x* activity at lower temperatures of around 250–350 °C. Besides, Cu–Al–MCM-41 catalyst also showed higher acetone oxidation than those of Cu–MCM-41, CuO/Al_2O_3 and CuO/SiO_2 catalysts in the entire temperature range. For higher temperature of above 400 °C, it was found that Cu–MCM-41 catalyst shows highest activity for the NO reduction but it shows less acetone incineration activity as compared to that of Cu–Al–MCM-41 catalyst. The study of simultaneous removal of NO and acetone solvent vapors using Cu–Al–MCM-41 and Cu–MCM-41 catalysts reveals the potential of using waste organic solvents from industry as the reducing agent of deNO*x* (SCR) process.

1. Introduction

Environmentally benign catalytic technology for reduce or eliminate the toxic gases from atmosphere is receiving considerable attention in recent years owing to its cleanness and highly efficient green process [1]. The emissions of nitrogen oxides (NO*x*) and volatile organic compounds (VOCs) are the subject of stringent legislation as a result of their adverse impacts on not only environment but also human health [2,3]. The large amount of waste organic solvents generated by the chemical manufacturing industries has always created environmental threats. For example, significant amounts of waste organic solvents from semiconductor and optoelectronic industries which contain isopropyl alcohol (IPA) and acetone as major components are facing problems of waste disposal due to limited treatment and disposal sites. Therefore the proper treatment of waste organic solvents is a crucial task for the environmental protection [4]. In this concern, the catalytic incineration technique has been commonly applied for waste solvent treatment [5,6]. However, the high installation cost of a catalytic incinerator as well as land availability may result in drawback of the catalytic incineration technique.

On the other hand, the increasing ozone and secondary aerosol formation in the atmosphere as well as the acid rain problems have raised further demand on the reduction of NO*x* from power plants and boilers. Thus the selective catalytic reduction (SCR) of NO*x* using ammonia or urea as the reducing agents has been extensively studied for the removal of NO*x* from the exhaust flue gases [7,8]. The cost of reducing agent in the SCR process usually accounts for about 30% of the total operation and maintenance cost [9]. Furthermore, for the deNO*x* from combustion of diesel engine, it has been extensively studied on using the hydrocarbons from fuel components such as CH_4, C_2H_4, C_3H_6 and C_3H_8 etc. as the reducing agents of SCR and is referred as the HC-SCR process [10–14]. Since the

* Corresponding author at: Researcher, Thermal Energy Storage (TES), CIC ENERGIGUNE, Energy Cooperative Research Centre, Parque Tecnológico, C/ Albert Einstein, 48, 01510 Miñano, Álava, Spain. Tel.: +34 945 297 108; mobile: +34 687318572.
E-mail addresses: mkarthik@cicenergigune.com, karthik_annauni@yahoo.co.in (M. Karthik).

0926-3373/$ – see front matter © 2013 Elsevier B.V. All rights reserved.
http://dx.doi.org/10.1016/j.apcatb.2013.08.014

property of many waste organic solvents is similar to that of the HCs used in the HC-SCR process, it may be possible to replace the HCs with waste organic solvents as the reducing agents. This not only saves the cost of reducing agents during SCR operation, but also minimizes the waste organic solvent treatment and disposal problems.

There is a little effort devoted to investigate the application of organic solvent vapors as the reducing agent in the deNO*x* process. For example, Lu and Wey [15] investigated the simultaneous removals of toluene and NO using transition metals impregnated activated carbon (AC)-based catalysts. However, the AC-based catalysts are very difficult to regenerate because of its poor thermal and chemical sensibility [16]. The M41S family of mesoporous materials discovered by researchers in Mobil Oil Corporation [17] have attracted great research attention because of its high specific surface area, uniform pore sizes with large pore diameters and high thermal & hydrothermal stability. Moreover, incorporation of Cu^{2+} ions into the framework of MCM-41 imparts both acidic and redox properties, which make such materials potentially interesting for catalytic oxidation and reduction reactions [18]. It is well known that copper is one of the cheapest and most active redox metals and thus copper supported catalysts have been widely studied for SCR deNO*x* reaction [12,19–21].

There are only limited reports on the simultaneous catalytic abatement of NO*x* and VOCs over copper containing MCM-41 catalysts. For example, Zhou et al. [22] have investigated the simultaneous reduction of NO*x* and oxidation of pyridine over copper supported zeolites and MCM-41 catalysts. They found that 2 wt.% copper supported MCM-41 (Cu/MCM-41) catalysts gave 37% of NO*x* conversion at very high temperature ca. 700 °C, but the catalytic activity of Cu/MCM-41 showed a little conversion ca. 5–10% at below 500 °C. Long and Yang [23] have demonstrated the catalytic activity of copper ion-exchanged Al–MCM-41 for the selective catalytic reduction of NO*x* by ethylene. They achieved about 25% and 85% conversions of NO*x* and ethylene, respectively, over copper ion-exchanged MCM-41 catalysts at 450 °C without water vapor.

The main goal of this paper is to evaluate the possibility of using waste organic solvent as a reducing agent for the removal of NO*x*. If this new technique is viable, then not only the cost of reducing agent (i.e. NH_3 or hydrocarbons (HCs)) can be eliminated but also the treatment of waste organic solvent can be approached simultaneously. Moreover, this work has great importance of dual catalytic reaction for the removal of two common pollutants in the gas phase. In the present study, the selective catalytic reduction of nitrogen monoxide (NO) using acetone solvent vapors (VOCs) as the reducing agent over Cu^{2+} and/or Al^{3+} incorporated MCM-41 catalysts have been investigated. The catalytic reactivity of the mesoporous catalyst is also compared with the copper oxide supported catalyst of CuO/SiO_2 and CuO/Al_2O_3 which are most commonly used in the catalytic incineration process [6,24–26]. The correlation between the catalytic reactivity of the material and the chemical nature of their active sites for VOC-SCR deNO*x* is also investigated and briefly discussed in this manuscript.

2. Experimental

2.1. Preparation of the catalysts

Hexagonal mesoporous Si–MCM-41, Cu–MCM-41 (50), Al–MCM-41 (50) and Cu–Al–MCM-41 (50) catalysts were synthesized by simple hydrothermal treatment method [20,21]. The molar composition of the gel mixture was SiO_2: 0.01–0.02 CuO: 0.01–0.02 Al_2O_3: 0.2 CTAB: 0.89 H_2SO_4: 120 H_2O (Si/Cu = 50, Si/Al = 50 and Si/Cu + Al = 50). Cetyltrimethylammonium bromide (CTAB) was employed as the structure-directing template in the synthesis. In a typical synthesis procedure, 21.2 g of sodium metasilicate nanohydrate dissolved in 80 ml DI water was combined with the appropriate amount of metal precursors like aluminium sulphate as aluminium source and/or copper nitrate for the copper source (dissolved in 20 ml DI water). The resulting mixture was stirred vigorously for 30 min. Then, approximately 40 ml of 4 N H_2SO_4 was added to the above mixture to bring down the pH to 10.5 with constant stirring to form a gel. After stirring, 7.28 g of CTAB (dissolved in 25 ml of DI water) was added slowly into the above gel mixture and the combined gel mixture was stirred for three additional hours. The resulting gel mixture was transferred into a Teflon coated autoclave and kept in an oven at 145 °C for 36 h. After cooling to the room temperature, the resultant solid was recovered by filtration, washed with DI water and dried in an oven at 110 °C for 6 h. Finally, the organic template was removed by using a muffle furnace in air at 550 °C for 10 h.

The SiO_2 (amorphous, 80 nm APS powder, 99.90%) and Al_2O_3 (powder, <10 micron) as reference catalyst supports was also tested for comparison. The CuO/SiO_2 and CuO/Al_2O_3 catalysts were prepared by a simple incipient wetness impregnation method as commonly employed for preparing Cu-based catalyst for catalytic incineration process [6,24–26]. The metal oxides were mixed with 0.05 M of copper (II) nitrate solution (15 ml per g of support) and stirred for 30 mints. The resulting solution was transferred into an evaporating dish and kept in an oven at 110 °C for 12 h. Then the fine grinded materials were calcined at 550 °C for 6 h.

2.2. Physicochemical characterization of the catalysts

Low angle powder X-ray diffraction patterns of calcined samples were recorded by using Rigaku X-ray diffractometer equipped with nickel-filtered CuKα (λ = 1.5405 Å) radiation. The diffractograms of the mesoporous samples were recorded in the 2θ range between 2° and 10° in steps of 0.6 degree with a count time of 60 s at each point. The specific surface area, specific pore volume and average pore diameter (BJH method) of the samples were measured by N_2 adsorption–desorption isotherms at 77 K using a surface area analyser (Micromeritics, ASAP 2000). All the samples were degassed for 6 h at 350 °C under vacuum (10^{-6} mbar) prior to the adsorption experiments. TEM images of the samples were observed with a JEOL JEM 1210 TEM instrument operated at 120 keV and the samples (5–10 mg) were ultrasonicated in ethanol and dispersed on carbon film supported on copper grids (200 mesh). The ^{27}Al MAS-NMR spectra of the mesoporous samples were recorded at room temperature using a BRUKER DSX 400 WB NMR spectrometer. The Larmor frequency was 104.1 MHz and aluminium chloride was used as external reference material for ^{27}Al MAS-NMR. The EPR spectra of the mesoporous samples were recorded at 77 K using a BRUKER spectrometer with operating resonance frequency of 9.6 GHz and field modulation of 100 KHz. The elemental copper in the samples were analyzed by a SCIEX ELAN 5000-Inductively Coupled Plasma-Mass Spectrometer (ICP-MS).

2.3. Catalytic performance test

The simultaneous catalytic reduction of NO and oxidation of acetone solvent vapors were carried out by a continuous flow reactor system as shown schematically in Fig. 1. The reactor system was vertical and down-ward flow type made up of a glass tube of 47 cm length and 2 cm internal diameter. The glass reactor was heated to the requisite temperature with a tubular furnace inserted with a thermocouple which controlled by a digital temperature controller. The source of NO gas was supplied from cylinder and diluted by a separate air stream. In the present study, acetone was chosen as a probe volatile organic compound because it is a common organic solvent used in semiconductor and optoelectronic industries. The

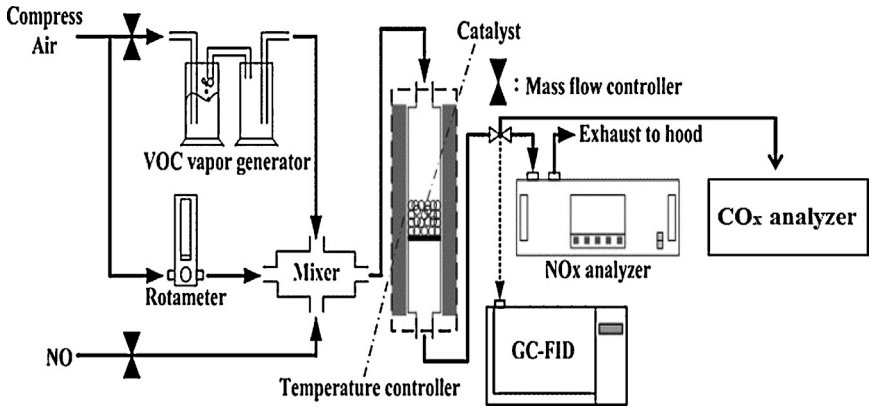

Fig. 1. Schematic representation of the experimental set-up for the VOCs-SCR of NO.

various inlet concentrations of acetone vapors were controlled by passing carrier gas through an impinger containing acetone and the impinger was kept in a constant-temperature controller maintaining at 4 °C.

A feed gas of reactant mixture containing 0.05 vol.% NO (500 ppm), 0.5 vol.% acetone (5000 ppm) and compressed air (balance) were passed through mass flow controllers to the reactor. The relative humidity in the compressed air was 35 ± 5% (25 °C and 1 atm). The total flow rate of the system was fixed at about 2000 cm^3/min (at 25 °C and 1 atm), which corresponded to a GHSV of 8500 h^{-1} (weight of the catalyst/total flow rate (W/F) = 0.03 g s cm^{-3}). About 1 g of the pelletized catalyst (16–30 mesh) was homogeneously mixed with small glass beads (2 mm i.d) which placed in the middle of the reactor and supported on either side with a thin layer of glass wool. Prior to each catalytic reaction, the catalysts were activated at 500 °C for 2 h. The inlet and outlet concentrations of NO and NO_2 (NO*x*) were monitored by an on-line NO*x*/SO*x* analyser (SIEMENS ULTRAMAT 23, Germany). However, due to the instrument limitation the intermediate product of N_2O was not measured. And because only negligible amounts of NO_2 were observed for all tests therefore in this study only the NO conversions were reported.

The inlet and outlet concentrations of acetone were analyzed by a gas chromatograph (SRI-8610C, USA) using capillary column (30 m) equipped with a flame ionization detector (FID). And the outlet concentrations of carbon dioxide (CO_2) and carbon monoxide (CO) from oxidation of acetone were also measured by a CO*x* metre (8760 IAQ-CALC metre). Carbon dioxide (CO_2) was found to be the major product and only negligible amount of CO was identified in this study. This may be due to that acetone is a simple structured organic compound.

3. Results and discussion

3.1. X-ray diffraction and BET analysis

Low-angle powder X-ray diffraction patterns of calcined mesoporous Si–MCM-41, Cu–MCM-41, Al–MCM-41 and Cu–Al–MCM-41 are depicted in Fig. 2. The XRD pattern of Si–MCM-41 exhibits a well ordered structure and the peaks are indexed on a hexagonal lattice which corresponding to (1 0 0), (1 1 0), (2 0 0) and (2 1 0) reflections [20,21]. After metals substitution, the intensities of (1 0 0) reflection are decreased and (1 1 0) and (2 0 0) reflection peaks are essentially merged into one broad peak. This can be ascribed to either partial loss of long range crystallographic order or formation of metal oxide species located inside the mesopores upon calcination at 550 °C [27,28].

The physicochemical parameters of all calcined samples derived from XRD and BET analysis are summarized in Table 1. As can be seen, CuO supported metal oxide catalysts show very less surface area compared to those of mesoporous catalysts. The average pore diameter of aluminium and copper substituted MCM-41 sample (Cu–Al–MCM-41) is almost similar to that of the Cu–MCM-41 sample, but the specific surface area of this sample is slightly higher than those of both Cu–MCM-41 and Al–MCM-41 samples. In addition, the average pore diameter of Al–MCM-41 sample is smaller than those of Cu–MCM-41 and Cu–Al–MCM-41. This could be due to the formation of some metal oxide clusters in the mesopores of Al–MCM-41 which may be partially blocking the pore mouth of the mesostructure [28,29]. Based on the XRD and BET results, it is proved that Cu^{2+} and/or Al^{3+} ions could be incorporated into the framework of MCM-41. And the textural characteristics of mesoporous samples were almost retained even after metals incorporation. The copper contents of the samples were determined by ICP-MS and the results are also presented in Table 1. The Cu–Al–MCM-41 has the least amount of Cu, 1.87% by wt. as compared to those of Cu–MCM-41 (3.18%), CuO/SiO_2 (5.06%) and CuO/Al_2O_3 (4.65%).

3.2. Transmission electron microscopy (TEM) analysis

In order to further confirm the structural features of these mesoporous materials, the synthesized materials were investigated by TEM analysis. The TEM images of all the calcined mesoporous

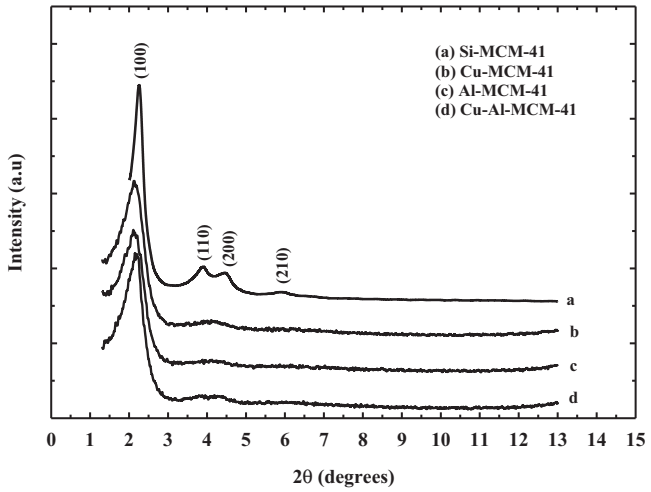

Fig. 2. XRD patterns of calcined mesoporous Si–MCM-41 and Cu and/or Al substituted MCM-41 materials.

Table 1
Physicochemical parameters of the catalysts.

Catalysts	Si/Al ratio	Si/Cu ratio	Copper Content (wt.%)	a_o (Å)	S_{BET} (m^2/g)	t_w (nm)	d_p, BJH (nm)	V_p (cm^3/g)
Si–MCM-41	–	–	–	45.10	1064	1.81	2.70	0.97
Cu–MCM–41	–	50	3.18	49.01	905	2.10	2.80	1.35
Al–MCM-41	50	–	–	39.82	1032	1.27	2.71	1.08
Cu–Al–MCM-41	100	100	1.87	39.82	1041	1.18	2.80	1.09
CuO/SiO_2	–	–	5.06	–	198	–	–	–
CuO/Al_2O_3	–	–	4.65	–	1.0	–	–	–

The lattice parameter (a_o) was calculated according to $a_o = 2\,d_{100}/\sqrt{3}$.
The wall thickness (t_w) was calculated according to $t_w = a_o - d_{P\,(BJH)}$.

materials are shown in Fig. 3. TEM image of Si–MCM-41 material clearly shows a well ordered long range hexagonal array of mesopores and this long range crystallographic highly ordered features of this material are also consistent with the results obtained from the low-angle XRD analysis. After metals incorporation, the partial loss of long range crystallographic order of the materials was observed as compared with those of pure Si–MCM-41. The ordered hexagonal arrangement of Cu–Al–MCM-41 material was better than that of mono-metal substituted MCM-41 like Cu–MCM-41 and Al–MCM-41. This is attributed to most of the Cu^{2+} and Al^{3+} ions predominantly substituted into the framework of MCM-41 rather than formation of some metal oxides upon calcination. The formation of metal oxides on mono-metal substituted MCM-41 was favoured and hence the structural arrangement of the material was decreased. Furthermore, the lattice fringes of metal species in MCM-41 samples can be clearly seen from the TEM image as shown in Fig. 3. The uniform porosity of the mesoporous materials revealed by TEM analysis is also consistent with the narrow pore size distribution (BJH) determined by N_2 adsorption–desorption measurements for all the calcined materials.

3.3. ^{27}Al magic angle spinning-nuclear magnetic resonance (MAS-NMR) spectroscopy

The ^{27}Al MAS-NMR spectra of calcined Al–MCM-41 and Cu–Al–MCM-41 materials are presented in Fig. 4. It can be seen that the signal observed at around 53 ppm can be assigned to tetrahedral coordinated aluminium and the signal appeared at around 0 ppm corresponds to octahedral coordinated aluminium [30]. The ^{27}Al MAS-NMR spectrum of calcined Al–MCM-41 material (Fig. 4a) shows a less intense peak at around 0 ppm (octahedral coordinated aluminium is ca. 5% and tetrahedral coordinated aluminium is ca. 95%). This peak can be ascribed to the formation of extra-framework aluminium species upon calcination and the presence of octahedral coordinated aluminium is most probably resulted from aluminium atoms interacting with water molecules [31]. On the other hand, the ^{27}Al MAS-NMR spectrum of calcined Cu–Al–MCM-41 material (Fig. 4b) exhibits only tetrahedral coordinated aluminium (**ca. 99%)** and this result clearly indicated that most of the aluminium species could be incorporated into the framework of MCM-41. From the NMR results, it is interesting to observe that the concomitant

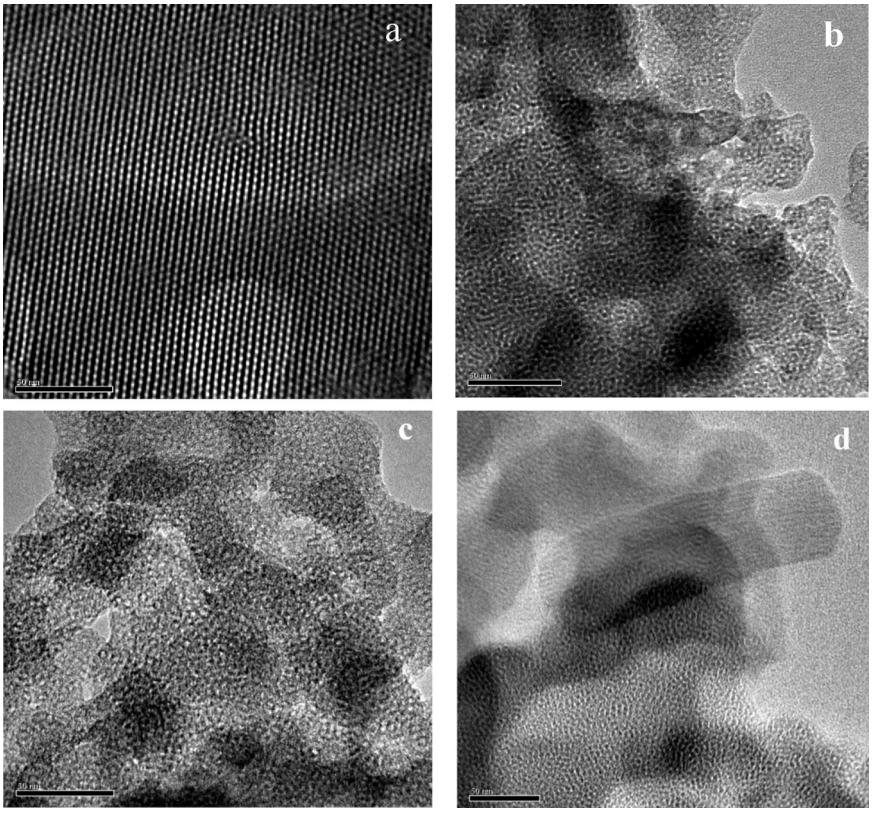

Fig. 3. TEM images of calcined mesoporous materials. (a) Si–MCM-41, (b) Cu–MCM-41 (50), (c) Al–MCM-41 (50) and (d) Cu–Al–MCM-41 (50). (Scale bar-50 nm).

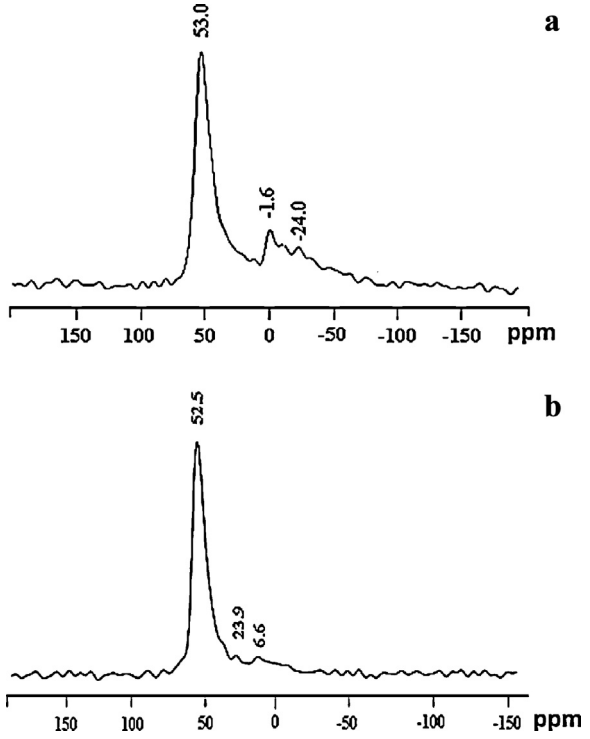

Fig. 4. ^{27}Al–MAS-NMR spectra of calcined mesoporous materials. (a) Al–MCM-41 and (b) Cu–Al–MCM-41.

presence of Cu^{2+} ions helps Al^{3+} ions predominantly substituted into the framework of MCM-41 [30].

3.4. Electron paramagnetic resonance (EPR) spectroscopy

The EPR spectra of calcined Cu–MCM-41 and Cu–Al–MCM-41 materials are shown in Fig. 5. The EPR spectrum of the Cu–Al–MCM-41 sample exhibits a well resolved four hyperfine lines with the spin Hamiltonian parameters $g_{||}$ in the range between 2.20 and 2.55 and $g_{\perp} = 2.05$. According to the literature data, the above range of the spin Hamiltonian parameters of the material can be ascribed to the presence of isolated Cu^{2+} ions with two types of coordination such as square pyramidal and square planer structure [32,33]. The four hyperfine lines and integrated intensity of the Cu–MCM-41 sample obtained by EPR are poorly resolved which may be due to the high

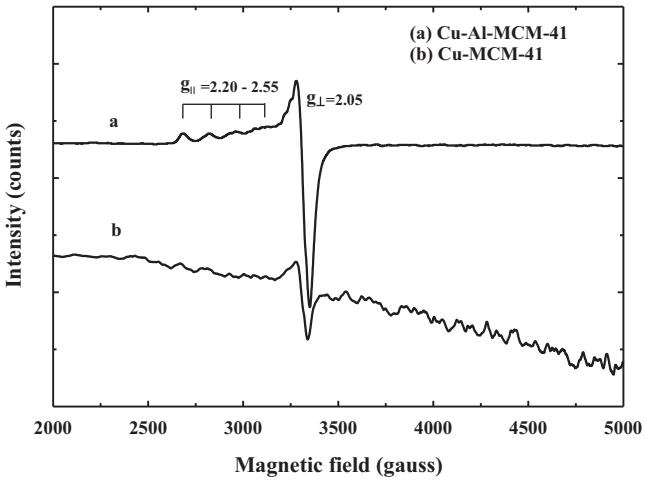

Fig. 5. EPR spectra of calcined mesoporous materials. (a) Cu–MCM-41 and (b) Cu–Al–MCM-41.

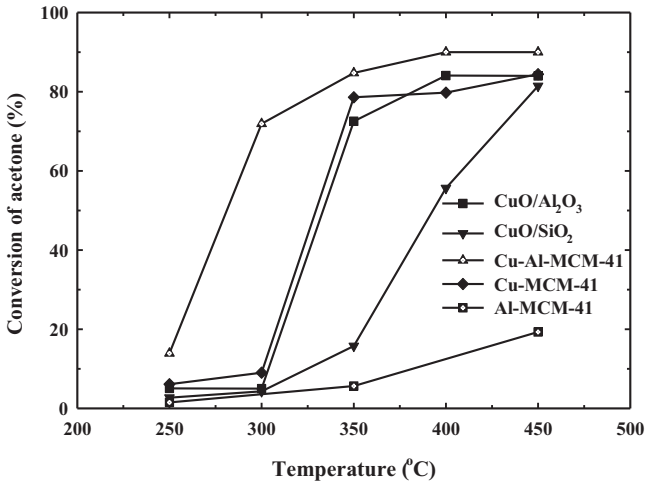

Fig. 6. Effect of reaction temperature on acetone conversion. GHSV: 8500 h^{-1}, NO: 500 ppmv and acetone: 5000 ppmv.

concentration of Cu^{2+} ions on the surface of the materials. In addition, the distances between Cu^{2+} ions on Cu–MCM-41 are so close, thus the EPR signals are decreased by the strong spin–spin interaction [32] and the formation of more CuO species also affect the EPR intensity. All the above results clearly suggest that the presence of aluminium in the framework promoted MCM-41 to stabilize a much large portion of isolated Cu^{2+} ions as compared to Cu–MCM-41 without aluminium [33]. Thus the most of the Cu^{2+} ions in the Cu–Al–MCM-41 are isolated and well dispersed on the surface of the mesoporous material.

3.5. Simultaneous oxidation of acetone and reduction of NO

3.5.1. Acetone oxidation

The acetone oxidation with the presence of NO as a function of reaction temperatures are shown in Fig. 6. The acetone conversion was recorded after 1 h of time-on-stream operation for each reaction temperature test. It is noticed that the acetone oxidation rate of the catalysts is in the order of Cu–Al–MCM-41 > Cu–MCM-41 ≥ CuO/Al_2O_3 > CuO/SiO_2 > Al–MCM-41. The bimetallic Cu–Al–MCM-41 catalyst exhibits a better acetone incineration activity than both Cu–MCM-41 and Al–MCM-41 in the entire temperature range. Since Al–MCM-41 without copper ions exhibits less activity, the presence of copper ions in the catalyst clearly play an important role for acetone incineration. On the other hand, Cu–Al–MCM-41 catalyst showed a higher acetone incineration activity than that of Cu–MCM-41 without aluminium ions. From the above observation, it is clear that the synergistic interaction between copper and aluminium ions in the Cu–Al–MCM-41 catalyst is a critical factor which may determine the performance of the catalyst.

In this study, silica (SiO_2) was used as a support because of its well-known inert character. It is expected that there is no interaction between silica and copper species in the CuO/SiO_2. Thus CuO/SiO_2 catalyst shows less acetone incineration activity as compared to that of CuO/Al_2O_3 catalyst. It has been previously reported that the CuO supported Al_2O_3 was the most active catalyst as compared to the CuO/SiO_2 for the catalytic incineration of volatile organic compounds [24,25]. The maximum acetone conversion of ca. 85% over CuO/Al_2O_3 catalyst was obtained at 400 °C (T_{max}) and then the acetone conversion was almost maintained with respect of temperature. This behaviour has been observed by several authors in the literature during the combustion of hydrocarbons on alumina supported Cu catalysts [24–26]. However, Cu–Al–MCM-41

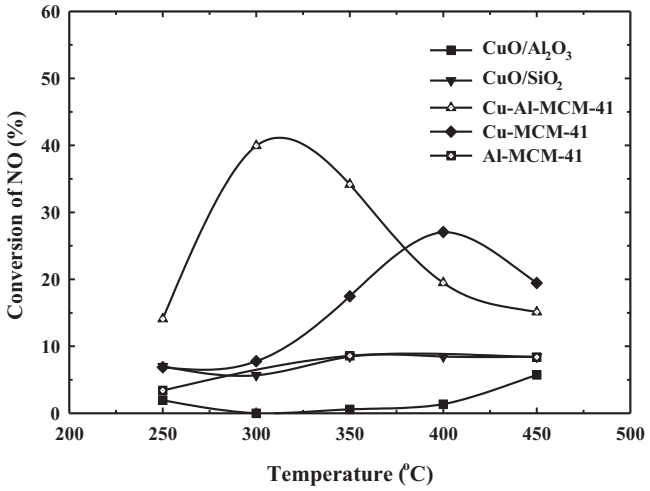

Fig. 7. Effect of reaction temperature on conversion of NO. GHSV: 8500 h^{-1}, NO: 500 ppmv and acetone: 5000 ppmv.

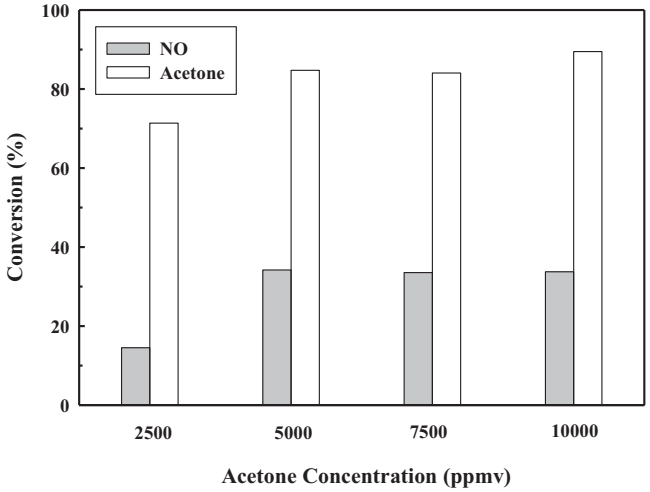

Fig. 8. Influence of acetone concentration on conversions of NO and acetone. Catalyst: Cu–Al–MCM-41; temperature: 350 °C, GHSV: 8500 h^{-1} and NO: 500 ppmv.

catalyst showed the better removal efficiency of acetone than that of CuO/Al_2O_3 catalyst. This result clearly indicate that the isolated well dispersed Cu^{2+} ions and tetrahedrally coordinated Al^{3+} ions within the framework of Cu–Al–MCM-41 could promote the activity of the catalyst [22,34–36]. Hence Cu–Al–MCM-41 catalyst had a higher activity for the simultaneous removals of NO and acetone solvent vapors as compared to the other catalysts. Based on the above results, it can be concluded that the simultaneous incorporation of Cu^{2+} and Al^{3+} ions into the framework of MCM-41 play an important promoting effect in the catalyst and hence it shows a higher acetone incineration activity than the other catalysts.

3.5.2. NO reduction

The simultaneous catalytic removal tests of NO and acetone solvent vapors were carried out over Cu and/or Al substituted MCM-41 as well as CuO supported metal oxide catalysts. The conversion of NO as a function of reaction temperature is illustrated in Fig. 7. The NO conversion was recorded after 1 h of time-on-stream operation for each reaction test. The NO conversion evaluated at 250–350 °C is in the order of Cu–Al–MCM-41 > Cu–MCM-41 > $CuO/SiO_2 \geq$ Al–MCM-41 > CuO/Al_2O_3. The NO conversion over Cu–Al–MCM-41 catalyst is increased with increasing reaction temperature, it reaches a maximum at 300 °C (T_{max}) and then decreases again. Beyond this optimum reaction temperature (300 °C), the gradual decrease in NO conversion at elevated temperature is observed which can be attributed to the simultaneous and rapid oxidation of acetone under excess oxygen condition. This similar behaviour has been observed on Cu–ZSM-5 zeolite as well-known catalyst for HC-SCR reaction [37–39]. On the other hand, the maximum NO conversion over Cu–MCM-41 catalyst was obtained at 400 °C (T_{max}) and then the conversion was decreased due to the simultaneous oxidation of acetone in the vapor phase as observed in Cu–Al–MCM-41 catalyst. From the results, it is very interesting to see that the presence of aluminium in Cu–Al–MCM-41 catalyst can play an important promoting effect because it is not only enhanced the catalytic activity but also reduced the T_{max} of the VOC-SCR deNO*x* reaction.

As can be seen from Fig. 7, Cu–Al–MCM-41 catalyst shows a much higher NO conversion at 250–350 °C than that of Cu–MCM-41 catalyst. Although Cu–MCM-41 catalyst was more active for NO reduction by acetone vapors in the reaction temperatures of 400–450 °C, but the maximum deNO*x* activity and acetone oxidation activity of Cu–MCM-41 was lower than that of Cu–Al–MCM-41 catalyst. The other catalysts of CuO/SiO_2, CuO/Al_2O_3 and Al–MCM-41 show less than 10% NO removal efficiencies. Thus the results clearly indicate that the isolated well dispersed Cu^{2+} ions and tetrahedrally coordinated Al^{3+} ions within the framework of Cu–Al–MCM-41 could promote the activity of the catalyst. Hence the Cu–Al–MCM-41 catalyst had a higher activity for the simultaneous removals of NO and acetone solvent vapors as compared to the other catalysts.

3.5.3. Effect of acetone concentration

For practical application, the inlet concentration of organic solvent vapors can be easily controlled via adjusting the waste solvent feed rate. Thus the effects of acetone inlet concentrations on the simultaneous removals of NO and acetone solvent vapors were tested over Cu–Al–MCM-41 catalyst and the results are shown in Fig. 8. It can be seen that the NO conversion was increased when increasing the acetone vapor concentration from 2500 to 5000 ppm and it reached maximum. And then the NO conversion maintained up to concentration of acetone ca. 10,000 ppm. Thus the excess presence of acetone vapors helps to promote the reduction of NO via the oxidation of itself. On the other hand, the acetone conversion also increases with the increasing concentration and it attained about 90% conversion at acetone vapors concentration of 10,000 ppm. This further proves the synergic effect under the presence of both NO and acetone solvent vapors. The above observation reveals that bifunctional Cu–Al–MCM-41 catalyst is a suitable candidate for the practical application in the wide-range concentrations of waste organic solvent treatment processes.

3.5.4. Stability of the catalyst

The time-on-stream study was conducted to assess the long term stability of catalysts and its effect on the simultaneous reduction of NO and oxidation of acetone, and also to assess the deactivation effect of the catalysts. The conversions of NO and acetone as a function of time-on-stream study were examined over Cu–Al–MCM-41 and the results are presented in Fig. 9. It was found that NO conversion on Cu–Al–MCM-41 catalyst was initially increased with time-on-stream operation up to 8 h and then slightly decreased, and finally stabilized at ca. 35% after 26 h of operation time. On the other hand, the acetone conversion was initially decreased with time-on-stream operation and then finally stabilized at ca. 78% after 26 h of operation time. From the results, it is evident that NO and acetone conversion over Cu–Al–MCM-41 catalysts almost remains the same up to 26 h. Meanwhile, it

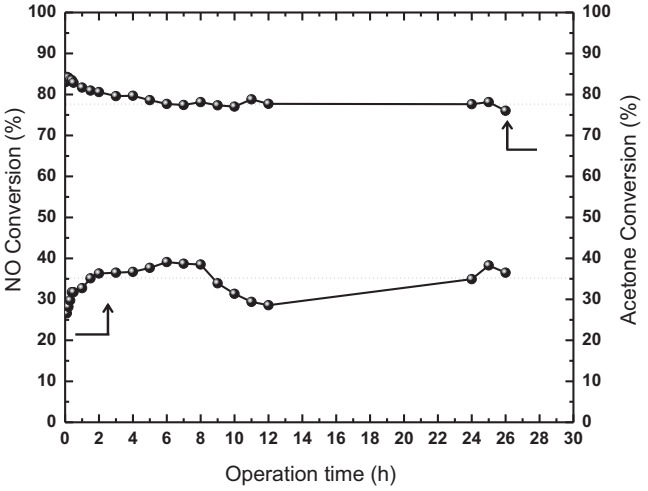

Fig. 9. NO and acetone conversion as a function of time-on-stream over Cu–Al–MCM-41 catalyst. Temperature: 350 °C, GHSV: 8500 h^{-1}, NO: 500 ppm and acetone: 5000 ppm.

is observed that the colour of Cu–Al–MCM-41 catalysts did not change even at the end of 26 h operation. Furthermore, Fig. S1 (Supplementary material) shows the N_2 adsorption–desorption isotherms of Cu–Al–MCM-41 before and after reaction on time-on-stream to understand the stability and textural meso-porosity of Cu–Al–MCM-41 catalyst. The specific surface area, average pore diameter and wall thickness of the catalyst before and after reaction are 1041 m^2/g, 2.8 nm and 1.18 nm and 915 m^2/g, 2.5 nm and 1.30 nm, respectively. The BET results indicate that the mesoporous nature and structural integrity of the catalyst is retained even after 26 h of reaction on time-on-stream. These results suggest that the unique mesoporous structures and medium acidity of the catalyst could play a key role in the simultaneous abatement of NO*x* and VOCs.

Supplementary material related to this article can be found, in the online version, at http://dx.doi.org/10.1016/j.apcatb.2013.08.014.

4. Conclusions

Bifunctional mesoporous Cu–Al–MCM-41 catalyst was synthesized by simple hydrothermal method. The experimental results clearly indicate that well dispersed and isolated Cu^{2+} ions present in the mesoporous Cu–Al–MCM-41 catalyst could act as an active redox centre in the simultaneous catalytic reduction and oxidation reaction. It is concluded that mesoporous Cu–MCM-41 as well as metal oxides such as CuO/Al_2O_3 and CuO/SiO_2 catalysts are less active for the simultaneous removals of NO and acetone vapors as compared to those of bifunctional Cu–Al–MCM-41 catalyst. Thus Cu^{2+} and Al^{3+} substituted MCM-41 was deliberated as an effective bifunctional catalyst for the selective reduction of NO and oxidation of acetone solvent vapors under excess of oxygen. The BET results indicate that the mesoporous nature and structural integrity of the catalyst is retained even after 26 h of reaction on time-on-stream. These results suggest that the unique mesoporous structures and medium acidity of the catalyst could play a key role in the simultaneous abatement of NO*x* and VOCs. Further detailed investigations of mesostructured Cu–Al–MCM-41 catalyst using other VOCs are required in order to draw a clear conclusion about its catalytic performance in the VOC-SCR deNO*x* process.

Acknowledgments

The authors gratefully acknowledge the financial support from the National Science Council of the Republic of China through grants NSC NO.: 95-2221-E-009-112-MY3.

References

[1] V.I. Parvulescu, P. Grange, B. Delmon, Catal. Today 46 (1998) 233–316.
[2] A. Fritz, V. Pitchon, Appl. Catal. B: Environ. 13 (1997) 1–25.
[3] D.P. Serrano, G. Calleja, J.A. Botas, F.J. Gutierrez, Ind. Eng. Chem. Res. 43 (2004) 7010–7018.
[4] F.I. Khan, A.K. Ghoshal, J. Loss Prev. Process Ind. 13 (2000) 527–545.
[5] K. Everaert, J. Baeyens, J. Hazard. Mater. B 109 (2004) 113–139.
[6] C-H. Wang, S.-S. Lin, C-L. Chen, H-S. Weng, Chemosphere 64 (2006) 503–509.
[7] M. Radojevic, Environ. Pollut. 102 (SI) (1998) 685–689.
[8] G. Busca, L. Lietti, G. Ramis, F. Berti, Appl. Catal. B: Environ. 18 (1998) 1–36.
[9] Y.-C. Lin, H. Bai, J. Chin. Inst. Environ. Eng. 12 (2002) 113–121.
[10] M.D. Amiridis, T. Zhang, R.J. Farrauto, Appl. Catal. B: Environ. 10 (1996) 203–227.
[11] Y. Traa, B. Burger, J. Weitkamp, Microporous Mesoporous Mater. 30 (1999) 3–41.
[12] H. Yahiro, M. Iwamoto, Appl. Catal. A: Gen. 222 (2001) 163–181.
[13] T. Wang, L. Li, N. Guan, Fuel Process. Technol. 108 (2013) 41–46.
[14] T. Chaieb, L. Delannoy, C. Louis, C. Thomas, Appl. Catal. B: Environ. 142–143 (2013) 780–784.
[15] C.-Y. Lu, M.-Y. Wey, Fuel Process. Technol. 88 (2007) 557–567.
[16] M. Guillemot, J. Mijoin, S. Mignard, P. Magnoux, Appl. Catal. B: Environ. 75 (2007) 249–255.
[17] C.T. Kresge, M.E. Leonowicz, W.J. Roth, J.C. Vartuli, J.C. Beck, Nature 359 (1992) 710–712.
[18] A.V. Kucherov, A.N. Shigapov, A.V. Ivanov, T.N. Kucherova, L.M. Kustov, Catal. Today 110 (2005) 330–338.
[19] G. Centi, S. Perathoner, Appl. Catal. A: Gen. 132 (1995) 179.
[20] C-K. Seo, B. Choi, H. Kim, C-H. Lee, C-B. Lee, Chem. Eng. J. 191 (2012) 331–340.
[21] A. Łamacz, A. Krztoń, G. Djéga-Mariadassou, Appl. Catal. B: Environ. 142–143 (2013) 268–277.
[22] J. Zhou, Q.H. Xia, S.C. Shen, S. Kawi, K. Hidajat, J. Catal. 225 (2004) 128–137.
[23] R.Q. Long, R.T. Yang, Ind. Res. Eng. Chem. 38 (1999) 873–878.
[24] E.M. Cordi, P.J. O'Neill, J.L. Falconer, Appl. Catal. B: Environ. 14 (1997) 23–36.
[25] C.H. Kim, J. Hazard. Mater. B 91 (2002) 285–299.
[26] G. Aguila, F. Gracia, J. Corte's, P. Araya, Appl. Catal. B: Environ. 77 (2008) 325–338.
[27] M. Karthik, A.K. Tripathi, N.M. Gupta, A. Vinu, M. Hartmann, M. Palanichamy, V. Murugesan, Appl. Catal. A: Gen. 268 (2004) 139–149.
[28] M. Karthik, L- Yi Lin, H. Bai, Microporous Mesoporous Mater. 117 (2009) 153–160.
[29] R.K. Jha, S. Shylesh, S.S. Bhoware, A.P. Singh, Microporous Mesoporous Mater. 95 (2006) 154–163.
[30] C.-L. Tsai, B. Chou, S. Cheng, J.-F. Lee, Appl. Catal. A: Gen. 208 (2001) 279–289.
[31] Z. Luan, C.-F. Cheng, H. He, J. Klinowski, J. Phys. Chem. 99 (1995) 10590–10593.
[32] A. Velu, L. Wang, M. Okazaki, K. Suzuki, S. Tomura, Microporous Mesoporous Mater. 54 (2002) 113–126.
[33] A.V. Kucherova, A.V. Ivanov, T.N. Kucherova, A.N. Shigapov, Kinet. Catal. 47 (2006) 881–890.
[34] Y. Wan, J. Ma, Z. Wang, W. Zhou, S.J. Kaliaguine, Appl. Catal. B: Environ. 59 (2005) 235–242.
[35] Y. Wan, J. Ma, Z. Wang, W. Zhou, S.J. Kaliaguine, J. Catal. 227 (2004) 242–252.
[36] C.-C. Liu, H. Teng, Appl. Catal. B: Environ. 58 (2005) 69–77.
[37] K.C.C. Kharas, Appl. Catal. B: Environ. 2 (1993) 207–224.
[38] J.O. Petunchi, W.K. Hall, Appl. Catal. B: Environ. 2 (1993) L17–L26.
[39] E. Kikuchi, K. Yogo, Catal. Today 22 (1994) 73–86.